JPEDAV (2011) 32:398–406
DOI: 10.1007/s11669-011-9916-8


# EMF Study of the Liquid Sb-Sn-Zn Alloys

*Tomasz Gancarz and Władysław Gąsior*

*(Submitted March 29, 2011; in revised form May 20, 2011)*

**The measurement of electromotive force (EMF) of concentration cells was applied to obtain zinc activity in ternary liquid Sb-Sn-Zn alloys in a $Zn_{liq}|(KCl\text{-}LiCl)_{eut} + ZnCl_2|(Sb\text{-}Sn\text{-}Zn)_{liq}$ galvanic cell. The measurements were carried out at temperatures from 723 up to 943 K for different Zn concentrations $X_{Zn}$ and for five constant ratios of Sn to Sb mole fractions, which were 1/3, 1, 3, 4 and 9. It was found out, that with increasing Sn concentration in the ternary alloys, the activity of Zn grew reaching the highest values for alloys of ratio Sn/Sb = 9 out of the ternary alloys examined. The observed straight-line changes of EMF matched a EMF = $A + B * T$ equation. The calculated coefficients served to obtain the activities and excess Gibbs free energy for selected temperatures 823 and 923 K.**

**Keywords** activity, electromotive force (EMF), Gibbs energy, Sb-Sn-Zn system, thermodynamic properties

## 1. Introduction

Multicomponent alloys based on the Sn-Zn eutectic belong to a group of materials with perspectives to apply in the industry of electronic systems apart from near-eutectic Ag-Sn-Cu alloys. Bismuth, indium and antimony are the most popular metals among the modifiers of soldering properties of the Sn-Zn eutectic.[1-5] However, the main interest of numerous research teams has so far concentrated on the measurements of many technological properties neglecting at the same time unquestionably difficult thermodynamic examinations. Hence, the experimental results of activities of components for many ternary alloys including the Sb-Sn-Zn ones are scarcely found in the scientific literature. Considering the above, such liquid alloys have been selected for experiments of thermodynamic properties. They, together with other equilibrium results, will derive the optimal thermodynamic parameters of phases occurring in the ternary alloys. It should be mentioned, that the $Sb_2SnZn$ intermetallic phase reveals an order-disorder transformation in the range of temperatures 498-513 K[6] and a peritectic transformation at 643 K. Its chemistry and some physical properties were examined by Scott already in 1973 due to its semi conductive properties and perspectives to be employed in optoelectronic.[7]

**Tomasz Gancarz** and **Władysław Gąsior**, Institute of Metallurgy and Materials Science PAS, 25 Reymonta Street, 30-059 Krakow, Poland. Contact e-mail: nmgancar@imim-pan.krakow.pl.

## 2. Experimental

The examinations of activity (partial free enthalpy) of zinc were carried out using the method of measurement of electromotive force (EMF) $E$ of a concentration cell, which may be schematically presented as follows:

$$Zn_{liq}|(KCl-LiCl)_{eut} + ZnCl_2|(Sb-Sn-Zn)_{liq} \quad \text{(Eq 1)}$$

The activity and partial molar Gibbs energy and partial excess Gibbs energy of zinc were calculated using the measurement results of EMF of cell (1) and the relationships given below:

$$\Delta G_{Zn} = -nFE = RT\ \ln(a_{Zn}) \quad \text{(Eq 2)}$$

$$a_{Zn} = \exp\left(\frac{-\Delta G_{Zn}}{RT}\right) \quad \text{(Eq 3)}$$

$$\Delta G^{ex}_{Zn} = -nFE - RT\ \ln X_{Zn} \quad \text{(Eq 4)}$$

In Eq 2-4, $n = 2$ is valence of $Zn^{2+}$ ions, $F$ stands for Faraday's constant, $E$ is value of the measured EMF of the cell, $R$ is the gas constant, $T$ denotes temperature, $a_{Zn}$ is zinc activity and $\Delta G_{Zn}$ and $\Delta G^{ex}_{Zn}$ are the partial molar Gibbs energy and partial excess Gibbs energy of zinc in liquid alloys Sb-Sn-Zn. The measurements were carried out in the cells shown schematically in Fig. 1.

A thermocouple was placed in an alumina tube between the electrodes in order to measure the temperature in the cell. To prepare the alloys, metals of high purity were used, 99.999% (Institute of Electronic Materials Technology). The cells were prepared in a glove-box under an Ar protective atmosphere, in which $O_2$ and $N_2$ concentrations were below 1 ppm. The monitoring unit was connected to a computer, which recorded the EMF charges and controlled the temperature on line.

All those factors, i.e. the purity of metals, atmosphere in the cell and the stability of temperature enabled the

obtaining of very precise and repeatable values of EMF for the examined alloys of the Sb-Sn-Zn system.

## 3. Results and Discussion

The measurements of Zn activity were carried out for five groups of alloys of constant ratio of mole fractions $n_{Sn}/n_{Sb}$, which was 1/3, 1, 3, 4 and 9 and the Zn concentration $X_{Zn}$ = 0.05 and from 0.1 and so on up to 0.9 (Fig. 2).

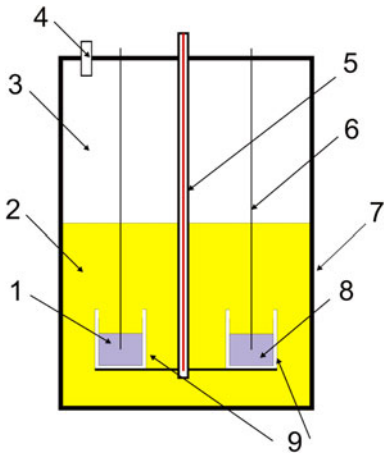


**Fig. 1** Scheme of measurement cell: 1, liquid Zn; 2, $(KCl + LiCl)_{eut} + ZnCl_2$ electrolyte; 3, argon atmosphere; 4, gas outlet ensuring the operation of cell at constant pressure; 5, thermocouple; 6, Ta lead wires; 7, quartz tube; 8, liquid Sb-Sn-Zn alloy; 9, crucible with $Al_2O_3$

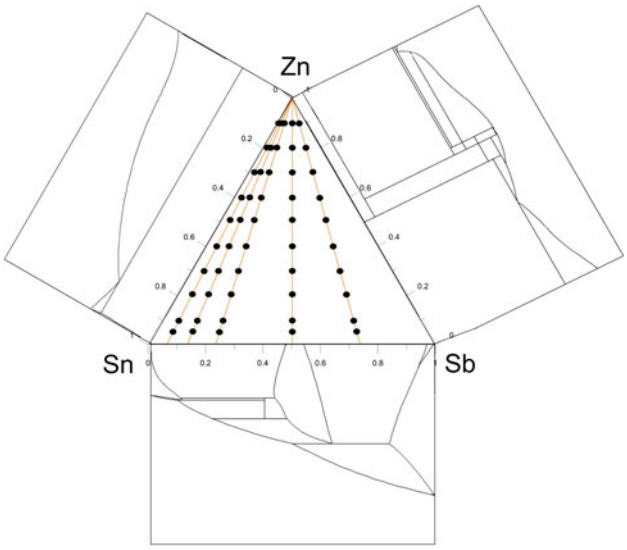


**Fig. 2** Composition of alloys, for constant Sn/Sb mole ratios with Zn additions

The temperature dependencies of EMF are presented in Fig. 3 and parameters $A$ and $B$ of straight lines fitted to experimental points, together with errors ($\delta A$ and $\delta B$) and the correlation coefficients $R^2$ are shown in Table 1.

The obtained relations of EMF on temperature allowed the calculation of Zn partial Gibbs energy $\Delta G_{Zn}$ and Zn activities at temperatures 823 and 923 K collected in Fig. 3-7 together with the Zn activity of binary Sn-Zn and Sb-Zn alloys[5,8] as well as Zn activity calculated based on a relation proposed by Muggianu et al.[9] $W_{i,j}$ interaction coefficients for the binary alloys are presented in Table 2, in which $X_i$ denotes mole fractions of the components.

The optimized thermodynamic parameters of Sb-Sn and Sn-Zn binary solutions from the COST 531 data base[8] and for Sb-Zn from the data base by Ohnuma and coworkers[5] were applied in the calculations of activity. In the following stage, values of Zn activity were calculated based on relations form Table 1 and Eq 2 for temperatures 823 and 923 K and they are presented in Fig. 8 and 9, respectively.

When analyzing the Zn activities in ternary Sb-Sn-Zn alloys in terms of dependence on content of Sn in the alloys (Fig. 4-8) it can be readily seen, that the activity of Zn increases with the increase of Sn concentration from its value in the Sb-Zn system, which reveals negative deviation from Raoult's law up to the activity for Sn-Zn system of positive deviations. In the case of solutions of the lowest Sn/Sb ratio (1/3), the measured Zn activities show negative deviations from 0 to 0.6 mole fractions Zn at 823 K. Optimized thermodynamic parameters from Ref 5 and 8 were used to calculate the activity of Zn with Muggianu model and the results of calculations show similar trends to experimental results (Fig. 4). In the solutions of ratio Sn/Sb = 1 and 3, deviations from the ideal Zn activity shift from negative to positive with increasing Zn content. Comparing the results obtained indirectly from the relation of Muggianu et al.,[9] satisfactory consistence of experimental and theoretical values was observed. The introduction of ternary interaction parameters into the optimization of thermodynamic properties of the liquid phase should improve the correlation between experimental values and the model values.

The dependencies of $a_{Zn}$ on $X_{Sn}$ in Sb-Sn-Zn alloys, shown in Fig. 9(a) and (b), refer to 10 alloys of Zn content from 0.05 up to 0.9 mole fraction. They were obtained using the least square method for temperatures 823 and 923 K. The resultant parameters from straight-line fits ($a_{Zn} = A + B * X_{Sn}$) to experimental data are presented in Table 3 together with errors of parameters and correlation coefficients.

The activities calculated from the straight lines (Table 3) proved to be consistent with the data of Ohnuma and COST 531 data base[5,8] for Sb-Zn and Sn-Zn systems shown in Fig. 10. Such a consistence lets us accept a linear change of Zn activity (Fig. 9a, b) with a change of Sb/Sn ratio.

The excess Gibbs energy values $\Delta G^{ex}_{Zn}$, presented in Fig. 11(a) and (b) at 823 and 923 K, were calculated directly from the measured values of EMF and Eq 4 for individual cross-sections of constant Sn/Sb ratio.

Figure 11(a) and (b) indicate a different course of Zn concentration dependence of the excess Zn free enthalpy

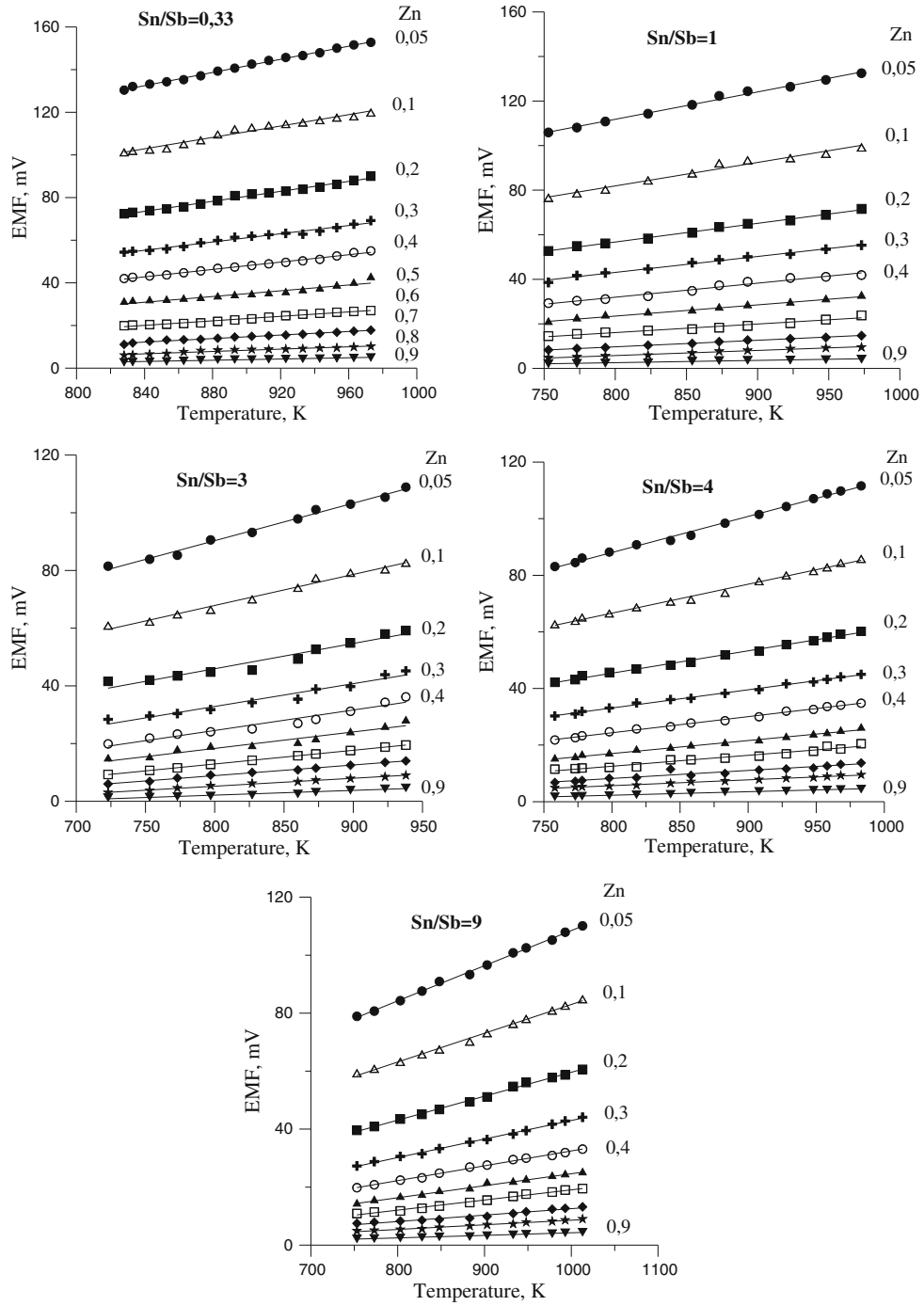


**Fig. 3** Dependence of EMF on temperature and Zn concentration for constant ratios Sn/Sb 0.33, 1, 3, 4, 9

for individual Sn/Sb ratios. The results of $\Delta G_{Zn}^{ex}$ obtained for ternary alloys are contained in the range between the limiting binary alloys SnZn and SbZn. As it is seen from Fig. 11(a) and (b), $\Delta G_{Zn}^{ex}$ weakly depended on temperature. It is for alloys with Sn/Sb ratio equal to 3 or higher positive and decreases with the increase of Zn content in the alloy. Such a course of concentration dependence is similar to the analogical relation for the Sn-Zn alloy. However, the $\Delta G_{Zn}^{ex}$ values for the alloys are slightly lower than these of the Sn-Zn alloy and they decrease together with the increase of Sb content in the alloy. In the case of alloys of Sn/Sb ratio 1 and 0.33, the

**Table 1 Parameters $A$ and $B$ of straight lines and correlation coefficient $R^2$, EMF for alloys of constant ratios Sn/Sb 0.33, 1, 3, 4, 9 with Zn additions**

| | EMF = $A + B * T$ | | | | |
|---|---|---|---|---|---|
| **Zn** | ***A*** | **δ*A*** | ***B*** | **δ*B*** | $R^2$ |
| Sn/Sb = 0.33 | | | | | |
| 0.050 | 3.0 | 2.1 | 0.1541 | 0.0023 | 0.997 |
| 0.100 | −9.3 | 5.3 | 0.1335 | 0.0059 | 0.973 |
| 0.200 | −24.7 | 2.9 | 0.1169 | 0.0032 | 0.990 |
| 0.300 | −26.0 | 3.5 | 0.0968 | 0.0039 | 0.978 |
| 0.400 | −29.8 | 2.1 | 0.0864 | 0.0023 | 0.990 |
| 0.500 | −26.0 | 2.1 | 0.0677 | 0.0054 | 0.919 |
| 0.600 | −24.2 | 1.7 | 0.0527 | 0.0018 | 0.983 |
| 0.700 | −22.4 | 1.2 | 0.0411 | 0.0014 | 0.985 |
| 0.800 | −16.1 | 1.6 | 0.0271 | 0.0018 | 0.941 |
| 0.900 | −9.0 | 0.7 | 0.0144 | 0.0008 | 0.961 |
| Sn/Sb = 1 | | | | | |
| 0.050 | 13.7 | 3.0 | 0.1227 | 0.0035 | 0.994 |
| 0.100 | −2.2 | 4.8 | 0.1052 | 0.0056 | 0.978 |
| 0.200 | −10.2 | 1.7 | 0.0837 | 0.0020 | 0.995 |
| 0.300 | −14.2 | 2.2 | 0.0716 | 0.0026 | 0.990 |
| 0.400 | −18.5 | 3.1 | 0.0630 | 0.0035 | 0.975 |
| 0.500 | −16.9 | 3.1 | 0.0505 | 0.0014 | 0.994 |
| 0.600 | −14.4 | 2.3 | 0.0382 | 0.0026 | 0.964 |
| 0.700 | −13.7 | 0.5 | 0.0293 | 0.0006 | 0.997 |
| 0.800 | −12.6 | 0.8 | 0.0229 | 0.0010 | 0.986 |
| 0.900 | −5.4 | 0.7 | 0.0100 | 0.0008 | 0.947 |
| Sn/Sb = 3 | | | | | |
| 0.050 | −13.5 | 3.7 | 0.1298 | 0.0044 | 0.991 |
| 0.100 | −18.1 | 3.8 | 0.1075 | 0.0045 | 0.986 |
| 0.200 | −24.1 | 6.2 | 0.0876 | 0.0074 | 0.946 |
| 0.300 | −30.5 | 4.9 | 0.0792 | 0.0059 | 0.958 |
| 0.400 | −32.2 | 4.9 | 0.0709 | 0.0058 | 0.949 |
| 0.500 | −27.3 | 4.9 | 0.0571 | 0.0050 | 0.942 |
| 0.600 | −25.1 | 0.1 | 0.0476 | 0.0001 | 1.000 |
| 0.700 | −20.6 | 0.7 | 0.0369 | 0.0008 | 0.996 |
| 0.800 | −16.8 | 0.6 | 0.0275 | 0.0008 | 0.994 |
| 0.900 | −10.9 | 1.2 | 0.0163 | 0.0015 | 0.939 |
| Sn/Sb = 4 | | | | | |
| 0.050 | −13.8 | 2.1 | 0.1273 | 0.0023 | 0.996 |
| 0.100 | −15.1 | 1.9 | 0.1022 | 0.0022 | 0.994 |
| 0.200 | −17.6 | 1.5 | 0.0787 | 0.0017 | 0.994 |
| 0.300 | −18.2 | 1.0 | 0.0642 | 0.0012 | 0.996 |
| 0.400 | −21.2 | 1.0 | 0.0570 | 0.0012 | 0.995 |
| 0.500 | −19.5 | 1.0 | 0.0457 | 0.0011 | 0.994 |
| 0.600 | −18.4 | 1.9 | 0.0386 | 0.0022 | 0.962 |
| 0.700 | −14.4 | 2.1 | 0.0283 | 0.0024 | 0.920 |
| 0.800 | −10.9 | 0.4 | 0.0206 | 0.0005 | 0.993 |
| 0.900 | −7.7 | 0.3 | 0.0124 | 0.0003 | 0.993 |
| Sn/Sb = 9 | | | | | |
| 0.050 | −12.7 | 1.6 | 0.1212 | 0.0018 | 0.998 |
| 0.100 | −16.4 | 1.6 | 0.0994 | 0.0018 | 0.997 |
| 0.200 | −22.8 | 1.4 | 0.0824 | 0.0015 | 0.997 |
| 0.300 | −20.9 | 0.9 | 0.0639 | 0.0010 | 0.997 |
| 0.400 | −18.7 | 0.9 | 0.0511 | 0.0010 | 0.996 |
| 0.500 | −16.8 | 0.9 | 0.0414 | 0.0011 | 0.993 |

**Table 1 Continued**

| Zn | EMF = $A + B * T$ | | | | |
|---|---|---|---|---|---|
| | $A$ | $\delta A$ | $B$ | $\delta B$ | $R^2$ |
| 0.600 | −16.0 | 0.9 | 0.0351 | 0.0010 | 0.991 |
| 0.700 | −9.8 | 1.2 | 0.0223 | 0.0014 | 0.964 |
| 0.800 | −7.4 | 0.5 | 0.0160 | 0.0006 | 0.987 |
| 0.900 | −4.6 | 0.3 | 0.0088 | 0.0004 | 0.983 |

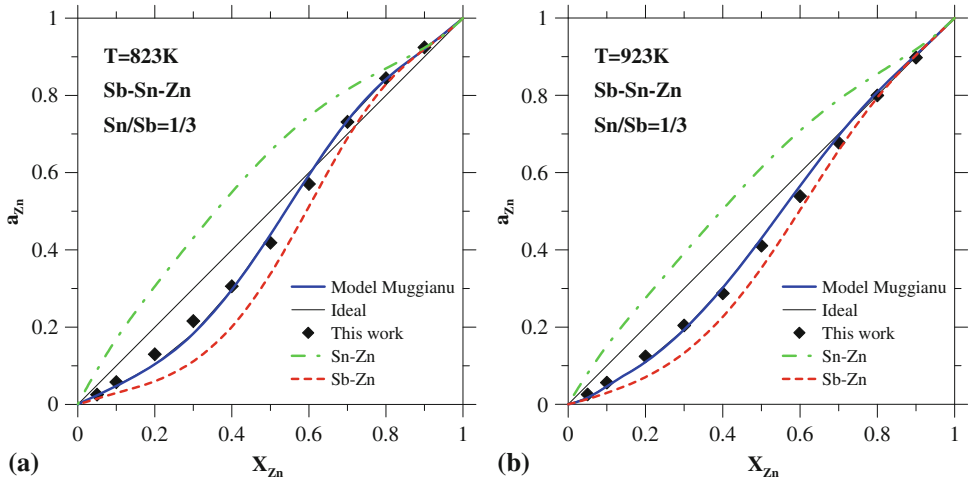


**Fig. 4** Zn activity in liquid ternary Sb-Sn-Zn alloys at 873 K (a) and at 923 K (b) for ratio Sn/Sb = 1/3 on the background of Zn activity in the binary Sb-Zn and Sn-Zn

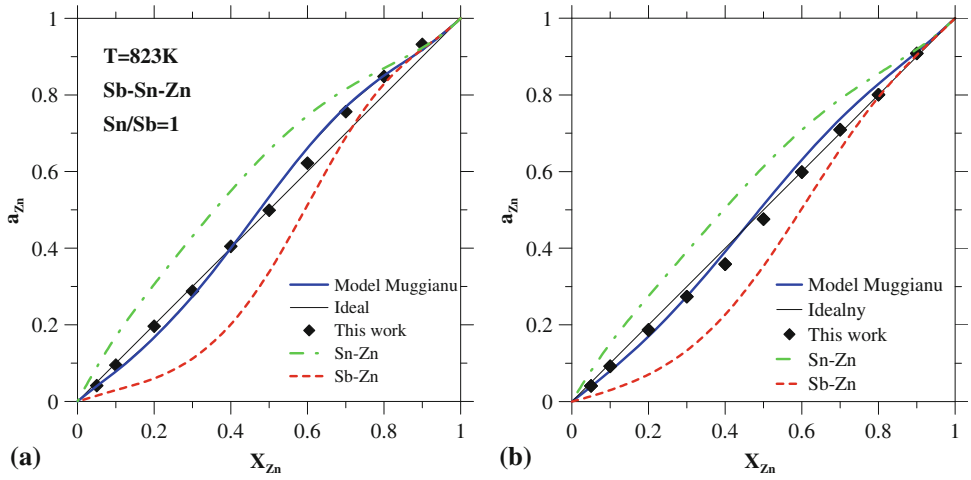


**Fig. 5** Zn activity in liquid ternary Sb-Sn-Zn alloys at 873 K (a) and 923 K (b) for Sn/Sb = 1 at the background of Zn activity in binary Sb-Zn and Sn-Zn systems

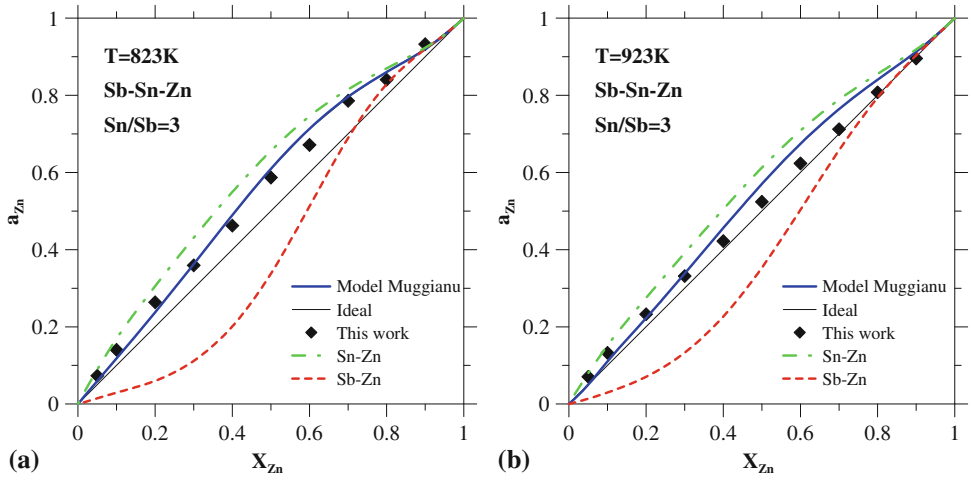


**Fig. 6** Zn activity in liquid ternary Sb-Sn-Zn alloys at 873 K (a) and 923 K (b) for Sn/Sb = 3 at the background of Zn activity in binary Sb-Zn and Sn-Zn systems

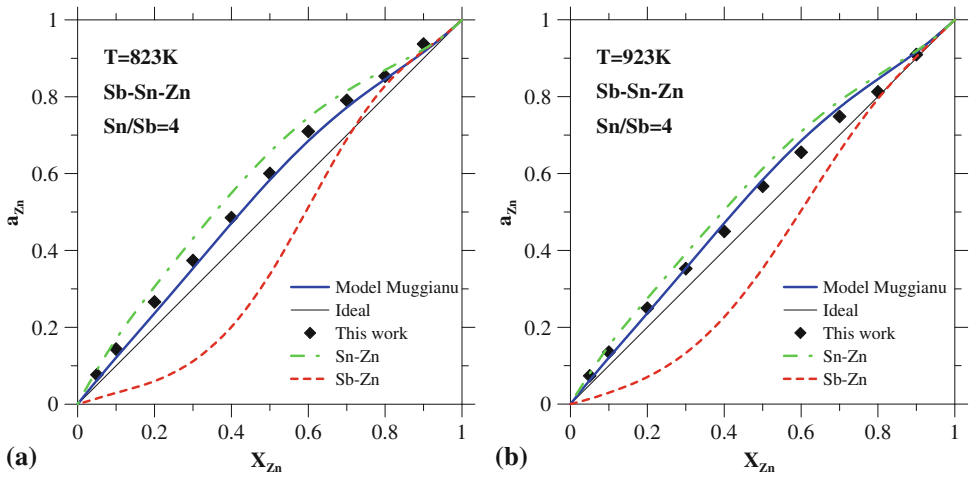


**Fig. 7** Zn activity in liquid ternary Sb-Sn-Zn alloys at 873 K (a) and 923 K (b) for Sn/Sb = 4 at the background of Zn activity in binary Sb-Zn and Sn-Zn

**Table 2 Interaction parameters of excess Gibbs energy of liquid Sb-Zn, Sb-Sn and Sn-Zn[5,8]**

| **Interaction coefficients for the binary alloys** |
|---|
| $W_{Sb,Zn} = (-11740.942 - 0.1283 * T) + (-427.582 - 0.809855 * T)(X_{Sb} - X_{Zn}) + (34440.943 - 33.59286 * T)(X_{Sb} - X_{Zn})^2$ |
| $W_{Sn,Zn} = (19314.64 - 75.89949 * T + 8.751396 * T * \mathrm{LN}(T)) + (-5696.28 + 4.20198 * T)(X_{Sn} - X_{Zn}) + (1037.22 + 0.98362 * T)(X_{Sn} - X_{Zn})^2$ |
| $W_{Sb,Sn} = (-5695.1 - 1.709 * T) + 782.6(X_{Sb} - X_{Sn}) + 1840.9(X_{Sb} - X_{Sn})^2$ |

$\Delta G_{Zn}^{ex} = f(X_{Zn})$ relation has a different course. The $\Delta G_{Zn}^{ex}$ values are negative for the Zn content from 0 to 0.6 mole fraction. Above $X_{Zn} = 0.6$, the $\Delta G_{Zn}^{ex}$ values are close to these for the alloys of higher Sn/Sb ratio. It can be distinctly seen, that with the increase of Sn/Sb ratio, the measured $\Delta G_{Zn}^{ex}$ values become higher, which is confirmed by the results for the Sn-Zn alloy whose $\Delta G_{Zn}^{ex}$ values are the higher.

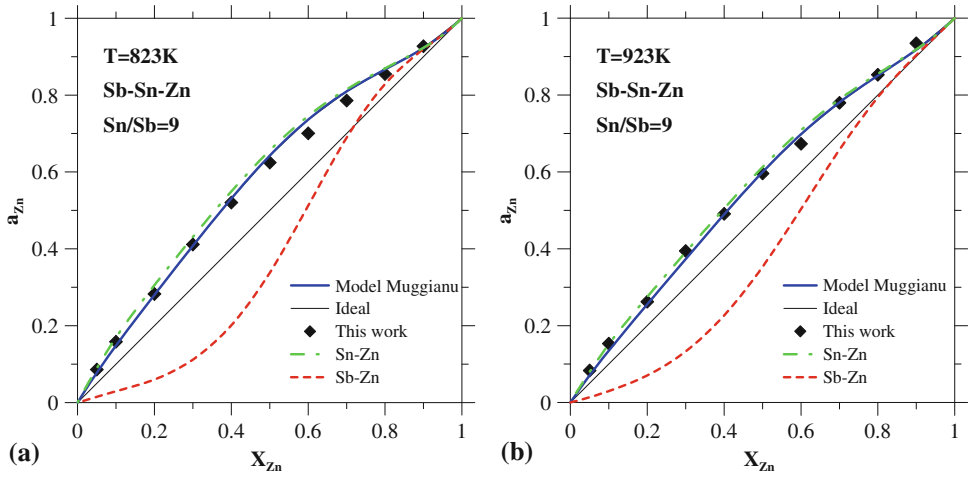


**Fig. 8** Zn activity in liquid ternary Sb-Sn-Zn alloys at 873 K (a) and 923 K (b) for Sn/Sb = 9 at the background of Zn activity in binary Sb-Zn and Sn-Zn

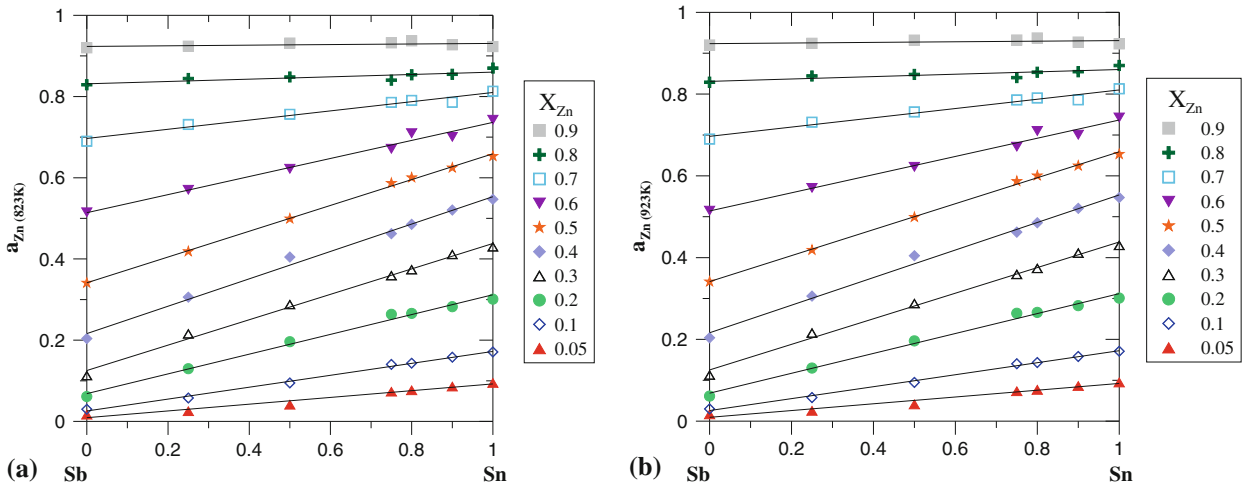


**Fig. 9** Activities of Zn in the Sb-Sn-Zn liquid alloys obtained from EMF data at 823 K (a) and 923 K (b) (symbols) together with these calculated using the COST 531 data base parameters for binary systems

## 4. Conclusions

The examination of Zn activity in liquid Sb-Sn-Zn alloys was carried out measuring the EMF of concentration cells for $X_{Zn}$ = 0.05, 0.1, 0.2, 0.3 0.4, 0.5, 0.6, 0.7, 0.8, 0.9 in the temperature range from 723 up to 943 K.

The increase of Zn activity was observed together with the growth of Sn content. In the alloys of Sn/Sb ratio equal to 1/3 at 823 K, for a lower Zn content, negative deviations were recorded, but when the Zn content increased, they changed into positive. In alloys of Sn/Sb ratio equal to 1 and 3, at 923 K, the Zn activity differed only slightly from that for the ideal solutions taking a little lower values for solutions of low Zn content, while for the rest a little higher ones. Positive deviations from the ideal behavior in the whole range of concentrations were observed in the alloys of Sn/Sb ratio equal to 3, 4, 9 at 823 and 923 K.

The Zn activity obtained based on the comparison of experimental and calculated from the relation of Muggianu, revealed, that the both sets of data are characterized by very small discrepancies, which may probably disappear when ternary interaction coefficients are introduced.

**Table 3 Parameters *A* and *B* of linear equations (Fig. 9a, b) describing the dependence of Zn activity on the Sn concentration in Sb-Sn-Zn liquid alloys at 823 and 923 K, correlation coefficients $R^2$ and errors of *A* and *B* (δ*A*, δ*B*)**

| $X_{Zn}$ | *A* | δ*A* | *B* | δ*B* | $R^2$ |
|---|---|---|---|---|---|
| $a_{Zn\ (823\ K)} = A + B * X_{Sn}$ | | | | | |
| 0.05 | 0.009 | 0.005 | 0.083 | 0.007 | 0.968 |
| 0.1 | 0.026 | 0.003 | 0.146 | 0.005 | 0.995 |
| 0.2 | 0.068 | 0.007 | 0.244 | 0.010 | 0.992 |
| 0.3 | 0.125 | 0.007 | 0.313 | 0.010 | 0.995 |
| 0.4 | 0.216 | 0.009 | 0.337 | 0.013 | 0.993 |
| 0.5 | 0.341 | 0.004 | 0.318 | 0.006 | 0.998 |
| 0.6 | 0.514 | 0.009 | 0.222 | 0.013 | 0.984 |
| 0.7 | 0.697 | 0.006 | 0.113 | 0.009 | 0.972 |
| 0.8 | 0.831 | 0.006 | 0.029 | 0.009 | 0.689 |
| 0.9 | 0.923 | 0.005 | 0.007 | 0.007 | 0.202 |
| $a_{Zn\ (923\ K)} = A + B * X_{Sn}$ | | | | | |
| 0.05 | 0.010 | 0.004 | 0.077 | 0.005 | 0.976 |
| 0.1 | 0.028 | 0.004 | 0.131 | 0.005 | 0.992 |
| 0.2 | 0.074 | 0.005 | 0.210 | 0.007 | 0.995 |
| 0.3 | 0.138 | 0.004 | 0.263 | 0.006 | 0.997 |
| 0.4 | 0.221 | 0.006 | 0.283 | 0.009 | 0.995 |
| 0.5 | 0.353 | 0.006 | 0.242 | 0.009 | 0.993 |
| 0.6 | 0.502 | 0.006 | 0.175 | 0.008 | 0.989 |
| 0.7 | 0.652 | 0.006 | 0.119 | 0.009 | 0.974 |
| 0.8 | 0.792 | 0.006 | 0.030 | 0.009 | 0.681 |
| 0.9 | 0.900 | 0.003 | 0.016 | 0.005 | 0.656 |

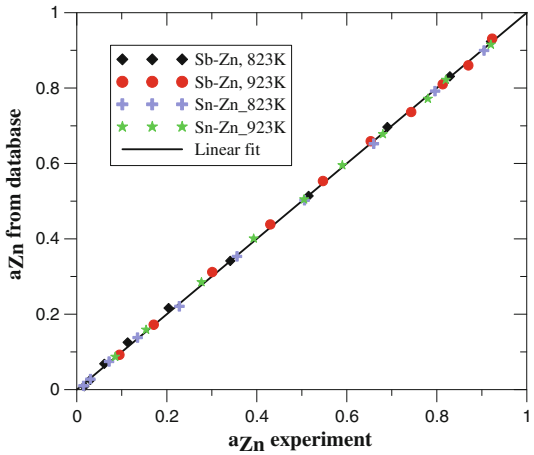


**Fig. 10** Dependence of experimental activity calculated from parameters of the straight lines Table 3 and the data of COST 531 data base for Sb-Zn and Sn-Zn systems at 823 K and 923 K

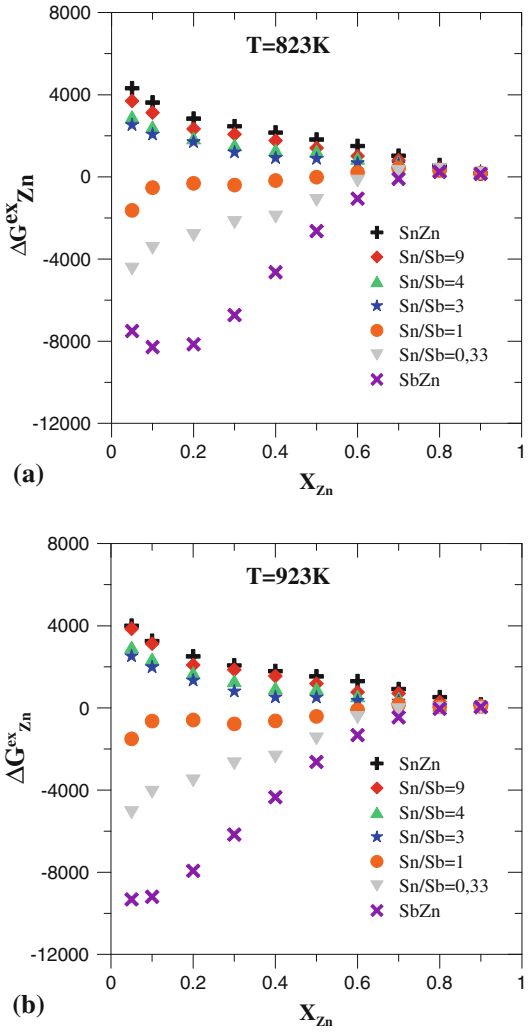


**Fig. 11** Excess Gibbs energy of zinc $\Delta G_{Zn}^{ex}$ calculated from measured EMFs for individual cross-sections Sn/Sb and for Sn-Zn and Sb-Zn liquid alloys (COST 531 data base) at 823 K (a) and 923 K (b), respectively



## References

1. K. Suganuma, Advances in Lead-Free Electronics Soldering, *Curr. Opin. Solid State Mater. Sci.*, 2001, **5**, p 55-64
2. Y. Kim, K. Kim, Ch. Hwang, and K. Suganuma, Effect of Composition and Cooling Rate on Microstructure and Tensile

Properties of Sn-Zn-Bi Alloys, *J. Alloys Compd.*, 2003, **352**, p 237-245
3. M. McCormack, S. Jin, and H.S. Chen, New Lead-Free, Sn-Zn-In Solders Alloys, *J. Electron. Mater.*, 1994, **23**, p 687-690
4. K. Lin and Ch. Shih, Wetting Interaction Between Sn-ZnAg Solders and Cu, *J. Electron. Mater.*, 2003, **32**, p 95-100
5. X.J. Liu, C.P. Wang, I. Ohnuma, R. Kainuma, and K. Ishida, Thermodynamic Assessment of the Phase Diagrams of the Cu-Sb and Sb-Zn Systems, *J. Phase Equilib.*, 2000, **21**(5), p 432-442
6. A. Tenga, J. Garcia-Garcia, A.S. Mikhaylishkin, B. Espinosa-Arronte, M. Anderson, and U. Haussermann, Sphalerite-Chalcopyrite Polymorphism in Semimetallic $ZnSnSb_2$, *Chem. Mater.*, 2005, **17**, p 6080-6085
7. W. Scott, Preparation and Some Properties of $ZnSnSb_2$, *J. Appl. Phys.*, 1973, **44**, p 5165-5166
8. A.T. Dinsdale, A. Watson, A. Kroupa, J. Vrestal, A. Zemanowa, and J. Vizdal, COST 531 Database for the Lead-Free Solders, 2008
9. Y.-M. Muggianu, M. Gambino, and L.P. Bross, Comparison Between Calculated and Measured Thermodynamic data of liquid (Ag, Au, Cu)-Sn-Zn alloys, *J. Chim. Phys.*, 1975, **72**, p 85-91